

The significance of diffusion tensor magnetic resonance imaging for patients with nasopharyngeal carcinoma and trigeminal nerve invasion

Tian Li, MD^a, Li Sheng, MD^a, Cui Chunyan, MD^a, He Haoqiang, MD^a, Peng Kangqiang, MD^a, Gong Xiao, MD^b, Liu Lizhi, MD^{a,*}

Abstract

To investigate the significance of diffusion tensor imaging (DTI) for patients with nasopharyngeal carcinoma (NPC) and trigeminal nerve invasion.

Fifty-two patients with NPC and unilateral infringement and 30 healthy controls were recruited for our study. Routine magnetic resonance imaging (MRI) and DTI were performed for all participants. Within-group and between-group comparisons of DTI metrics, including fractional anisotropy (FA) and the apparent diffusion coefficient (ADC) of the third (V3) branch of the bilateral trigeminal nerves of all participants, were carried out.

The FA and ADC values on the affected sides of patients revealed a significant decrease and increase, respectively, when compared with those on the unaffected sides of patients and the healthy controls ($P=0.000$ for all), whereas there were no significant differences in DTI metrics between both sides of healthy controls or between the unaffected sides of patients and the healthy controls ($P=0.930, 0.580, 0.095,$ and $0.360,$ respectively). The decreasing FA rate on the affected sides of patients correlated negatively with the increasing ADC rate ($r=-0.675, P=0.000$).

DTI can quantitatively evaluate microstructural abnormalities of the V3 branch of the trigeminal nerve in patients with NPC, which is important for the early detection of trigeminal nerve invasion to achieve a precise T classification, assess prognosis, and guide treatment.

Abbreviations: ADC = apparent diffusion coefficient, AJCC = the American Joint Committee on Cancer, DTI = diffusion tensor imaging, FA = fractional anisotropy, MRI = magnetic resonance imaging, NPC = nasopharyngeal carcinoma, ROIs = region of interests, SD = standard deviation, T1WI = T1 weighted image, TFE = turbo field echo, TN = trigeminal neuralgia.

Keywords: diffusion tensor imaging, magnetic resonance imaging, nasopharyngeal carcinoma, nerve invasion, trigeminal nerve

1. Introduction

Nasopharyngeal carcinoma (NPC) is endemic in Southeast Asia, and especially in the southern provinces of China.^[1] The

occurrence rate of cranial nerve invasion in patients with NPC ranges from 8% to 12.4%,^[2,3] in which trigeminal nerve invasion, and especially third (V3) branch invasion, is relatively common.^[4,5]

The objectives of clinical staging for malignant tumors are to predict prognosis, guide treatment, evaluate efficacy, and facilitate comparisons and exchanges of data and experiences among different centers.^[6] According to the widely used seventh edition of the American Joint Committee on Cancer (AJCC) staging system, patients with NPC and cranial nerve invasion are defined as stage T4, which seriously affects the prognoses of patients.^[5,7,8]

Magnetic resonance imaging (MRI) has proved to be a valuable tool in the assessment of cranial nerve invasion in patients with NPC. However, routine MR images evaluate cranial nerve invasion by assessing morphological changes of the nerve, such as neuroforaminal enlargement and the occurrence of local soft tissue. The value of routine MR images is quite limited in the assessment of abnormalities of the nerve microstructure resulting from cranial nerve impairment, possibly leading to a missed diagnosis of nerve invasion, and consequently to an incorrect T classification.

Diffusion tensor imaging (DTI) is a functional MRI technique that has certain advantages over routine MRI in showing microstructural changes in nerves resulting from neural damage. Fractional anisotropy (FA) and the apparent diffusion coefficient (ADC) are important quantization parameters. DTI has been widely used in the etiologic identification of trigeminal neuralgia

Editor: Laszlo Geza Boros.

Funding: This work was supported by the Natural Science Foundation of Guangdong Province, China (No. 2016A030310464), Medical Science and Technology Research Foundation of Guangdong Province (No. A2016328), the National Natural Science Foundation of China (No. 81572652).

TL and LS contributed equally to this work.

The authors have no conflicts of interest to disclose.

^a Department of Radiology, Sun Yat-sen University Cancer Center, State Key Laboratory of Oncology in South China, Collaborative Innovation Center for Cancer Medicine, ^b Department of Medical Statistics and Epidemiology, School of Public Health, Sun Yat-sen University, Guangzhou, Guangdong, People's Republic of China.

* Correspondence: Liu Lizhi, Department of Radiology, Sun Yat-sen University Cancer Center, State Key Laboratory of Oncology in South China, Collaborative Innovation Center for Cancer Medicine, 651 Dongfeng Road East, Guangzhou, Guangdong 510060, People's Republic of China (e-mail: lizhiliuabc@163.com).

Copyright © 2017 the Author(s). Published by Wolters Kluwer Health, Inc. This is an open access article distributed under the Creative Commons Attribution-NoDerivatives License 4.0, which allows for redistribution, commercial and non-commercial, as long as it is passed along unchanged and in whole, with credit to the author.

Medicine (2017) 96:6(e6072)

Received: 18 October 2016 / Received in final form: 22 December 2016 /

Accepted: 16 January 2017

<http://dx.doi.org/10.1097/MD.0000000000006072>

(TN). The practical value of DTI in patients with NPC and trigeminal nerve invasion has not been reported.

Hence, in the present study, we recruited a group of patients with unilateral infringed NPC and a group of healthy controls and analyzed differences in DTI parameters of the V3 branch of the trigeminal nerve in both groups to lay the foundation for a new assessment model based on DTI for patients with NPC and trigeminal nerve invasion. Our findings may be particularly important for improving the precision of the T classification of NPC, scientifically evaluating prognosis, and guiding treatment.

2. Methods

2.1. Patients

This study was approved by the institutional review board of our hospital and the experiments were conducted with the understanding and written consent of each participant.

From December 2015 to March 2016, 52 consecutive patients (37 men, 15 women, mean age \pm standard deviation [SD]: 45.8 ± 9.2 years) with newly diagnosed, untreated NPC were included in our study. All patients had a pretreatment evaluation that consisted of a complete history, physical and neurologic examinations, MRI scan of the neck and nasopharynx, chest radiography, and abdominal sonography. For all patients, the lesions in the nasopharynx were invaded unilaterally, and no conclusive evidence of trigeminal nerve invasion was detected on routine MR images. According to the AJCC (seventh edition) staging system, all patients were classified as T3.

We also enrolled 30 healthy controls with well-matched age and sex compositions. All of them underwent an MR scan of the neck and nasopharynx during the same period as the enrolled patients, and those with any lesions in the head and neck were excluded.

2.2. MRI Acquisition

Subjects lay supine on the bed of a 3-T MRI scanner (Achieva 3.0T; Philips Medical Systems, Best, The Netherlands) with their head and neck immobilized in a tight-fitting joint head and neck coil. After routine MRI, each subject underwent functional and morphological MRI.

Functional sequence: The median sagittal T1 weighted image (T1WI) was scanned first for localization of the slice position for the DTI sequence, followed by coronal scanning, which included the parapharyngeal space, masticator space, and pterygopalatine fossa. The DTI data acquisition was performed with a single-shot spin-echo planar-echo pulse sequence; the scanning parameters were as follows: echo time = 88 milliseconds, repetition time = 9000 milliseconds, flip angle = 90° , voxel size = $1.8 \text{ mm} \times 1.8 \text{ mm} \times 1.5 \text{ mm}$, matrix size = 100×100 , field-of-view = $180 \text{ mm} \times 180 \text{ mm}$, slice thickness = 1.5 mm, and interslice gap = 0. Diffusion gradients were applied along 15 independent orientations with $b = 1000 \text{ seconds/mm}^2$ after the acquisition of $b = 0 \text{ seconds/mm}^2$ (b_0) images (number of excitations: 2, acquisition time: 5 minutes and 29 seconds).

Morphological sequence: A turbo field echo (TFE) sequence was applied with the scanning parameters as follows: echo time = 9 milliseconds, repetition time = 527 milliseconds, flip angle = 8° , voxel size = $0.7 \text{ mm} \times 0.7 \text{ mm} \times 0.7 \text{ mm}$, matrix size = 328×322 , field-of-view = $230 \text{ mm} \times 230 \text{ mm}$, slice thickness = 0.7 mm, interslice gap = -0.7, number of excitations: 3, and acquisition time: 1 minute and 42 seconds.

2.3. Data processing

The data were processed using the Fibertrack and Diffusion software in the Extended MR Workspace.

The FA image could be derived from the DTI sequence and fused with the TFE images. The DTI metrics were calculated from the fusion model. First, the starting point where the V3 branch of the trigeminal nerve departs from the foramen ovale was located and the point that was 3 mm from the starting point was then found; thus, a three-dimensional tractography image of the V3 branch of the trigeminal nerve was generated, and the FA and ADC values of the nerve were derived automatically. The same method was applied to obtain DTI metrics of the contralateral trigeminal nerve. The DTI metrics of each nerve were obtained twice, and the average was the final result.

2.4. Statistical analysis

All DTI metrics are expressed as the mean \pm SD. Mean FA and ADC values were compared between the affected and unaffected sides in the same patients and between the right and left sides in the same healthy control using the Wilcoxon signed-rank test; comparisons of DTI metrics between patients and healthy controls were determined using the Mann-Whitney test. All tests were 2-tailed, and $P < 0.05$ indicated a significant difference. Spearman correlation analysis was used to assess the correlation between the decreasing FA rate and increasing ADC rate in the V3 branch of the trigeminal nerve on the affected side. All statistical calculations were performed with SPSS 17.0 software (SPSS, Inc., Chicago, IL).

3. Results

The data were not normally distributed and thus were analyzed using a nonparametric test. For all patients and healthy controls, the V3 branches of the trigeminal nerves were clearly visualized on both sides. The FA values of the nerves were significantly decreased on the affected side (mean \pm SD: 0.50 ± 0.19) compared to the unaffected contralateral side in patients (0.55 ± 0.20) ($P = 0.000$). ADCs of the nerves were remarkably increased on the affected side (mean \pm SD: $1.06 \pm 0.45 \times 10^{-3} \text{ mm}^2/\text{s}$) when compared to those on the unaffected contralateral side in patients ($0.89 \pm 0.42 \times 10^{-3} \text{ mm}^2/\text{s}$) ($P = 0.000$) (Fig. 1A and B). There were no significant differences in FA or ADC values of the nerves between the right side (mean \pm SD: 0.58 ± 0.18 ; $0.86 \pm 0.38 \times 10^{-3} \text{ mm}^2/\text{s}$) and left side in healthy controls (0.58 ± 0.20 ; $0.86 \pm 0.40 \times 10^{-3} \text{ mm}^2/\text{s}$) ($P = 0.93$ and 0.58 , respectively) (Fig. 2A and B). Furthermore, FA values of the nerves revealed an obvious decrease on the affected side in patients when compared to the FA values of healthy controls (mean \pm SD: 0.50 ± 0.19 vs 0.58 ± 0.18) ($P = 0.000$), whereas the ADCs of the nerves were found to increase remarkably on the affected side in patients, in contrast with the findings in healthy controls (mean \pm SD: $1.06 \pm 0.45 \times 10^{-3} \text{ mm}^2/\text{s}$ vs $0.86 \pm 0.39 \times 10^{-3} \text{ mm}^2/\text{s}$) ($P = 0.000$). The differences in the FA and ADC values of the nerves between the unaffected sides in patients and the healthy controls were not statistically significant (mean \pm SD: 0.55 ± 0.20 vs 0.58 ± 0.18 , $P = 0.095$; and $0.89 \pm 0.42 \times 10^{-3} \text{ mm}^2/\text{s}$ vs $0.86 \pm 0.39 \times 10^{-3} \text{ mm}^2/\text{s}$, $P = 0.360$, respectively). All comparative results are shown in Tables 1–4.

The decreasing FA rate of the nerves on the affected sides in patients was significantly negatively correlated with the increasing ADC rate ($r = -0.675$, $P = 0.000$) (Fig. 3).

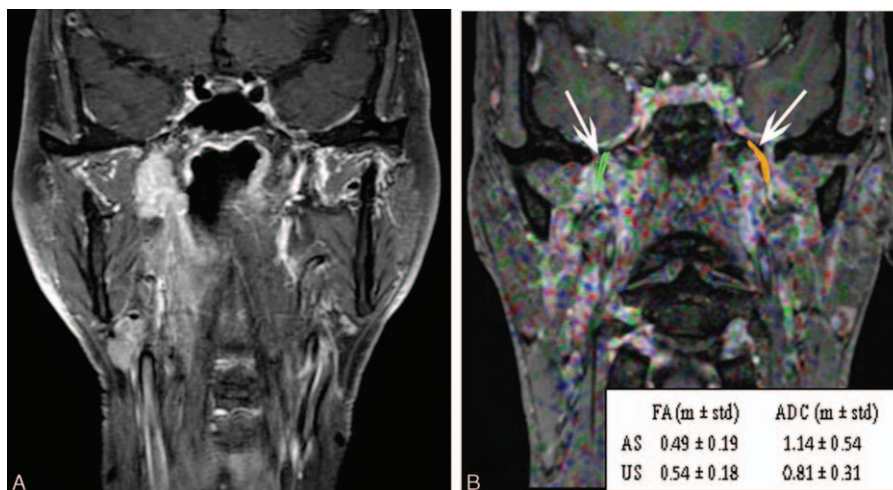


Figure 1. A routine MR image and fused diffusion tensor image with turbo field echo (TFE) sequence images of a 45-year-old man with nasopharyngeal carcinoma with a T3 classification. (A) Routine coronary magnetic resonance images with fat suppression and contrast enhancement show a nasopharyngeal lesion that has invaded the right parapharyngeal space without clear evidence of invasion of the V3 branch of the trigeminal nerve. (B) A fused image from DTI and TFE sequence. Diffusion tensor tractography images of the V3 branches of the bilateral trigeminal nerves were generated (white arrows). According to the metrics, FA values were decreased remarkably on the affected side (AS) compared to those on the unaffected side (US), and the ADC values were increased remarkably on the affected side compared to those on the unaffected side.

4. Discussion

Patients with NPC and cranial nerve invasion are relatively common and are classified as stage T4 according to the seventh edition of the AJCC staging system, mainly because of the high risk of distant metastasis.^[5,8] Cranial nerve invasion in NPC is a gradual process. Initially, the nerves are enveloped and compressed with pathological changes of demyelination and axonal degeneration, followed by direct invasion and destruction of the cranial nerves by tumor tissue, resulting in fibrosis and interruption of the nerve tracts as well as a local soft tissue mass.

MRI, with its superior soft tissue contrast resolution and multiplanar imaging capability, plays an important role in evaluating cranial nerve invasion in patients with NPC.^[4]

However, cranial nerve invasion is evaluated on routine MR images by detecting enlargement of the neural foramen or a local soft tissue mass. Additionally, an obvious shadow with abnormal signal intensity or abnormal enhancement in the contrast examination of the nerve line areas may exist. The value of routine MRI in revealing abnormalities of the nerve microstructure is extremely limited; it might result in some patients with NPC and early cranial nerve invasion being underestimated and downgraded in terms of T classification, affecting the scientific assessment of their prognoses and treatment decision-making.

DTI is a new imaging technique derived from diffusion-weighted imaging; it quantifies the amount of nonrandom water diffusion within tissues and provides unique in vivo information about pathological processes that affect water molecule diffusion

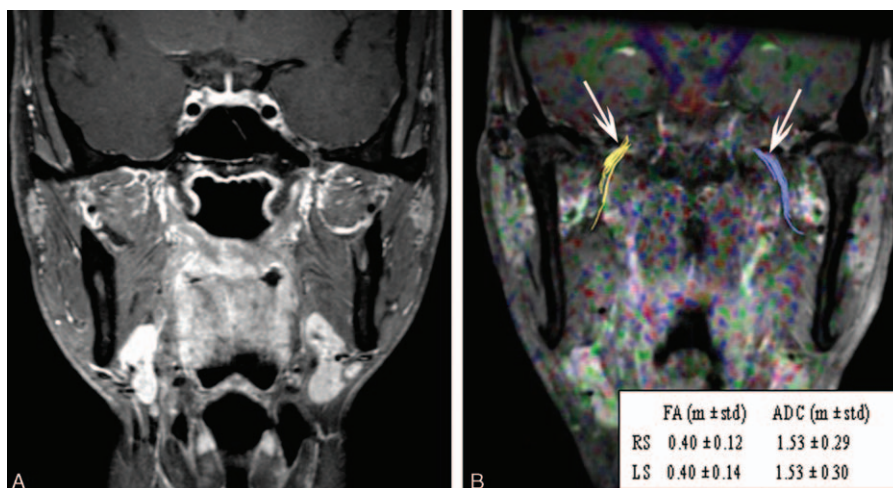


Figure 2. A routine MR image and fused DTI and turbo field echo (TFE) sequence images of a 42-year-old man who was a healthy control. (A) Routine coronary magnetic resonance images with fat suppression and contrast enhancement show no lesion in the nasopharynx or paranasopharyngeal space. (B) A fused DTI and TFE sequence image. Diffusion tensor tractography of the V3 branch of the trigeminal nerve was generated bilaterally (white arrows). The FA and ADC values showed no significant difference between the right side (RS) and the left side (LS).

Table 1**Comparison of FA and ADC values of V3 branch of the trigeminal nerve between both sides in patient group (n=52, mean±STD).**

	FA	ADC ($\times 10^{-3}$ mm ² /s)
Affected side	0.50±0.19	1.06±0.45
Unaffected side	0.55±0.20	0.89±0.42
Z	-6.275	-6.275
P	0.000	0.000

ADC=apparent diffusion coefficient, FA=fractional anisotropy, STD=standard deviation.

as a result of microstructural damage, which is out of the question on routine MRI.^[9,10] Two important parameters, FA and ADC, reflect the degree of direction-dependent diffusion and the free diffusion of water molecules, respectively. Therefore, degeneration or damage to neural fiber tracts is expected to lead to decreased FA (loss of diffusion directionality) and an increased ADC (loss of myelin and axonal membranes). In 2007, Herweh et al^[11] initially attempted to apply DTI to patients with TN and found that in patients with TN, FA values of the trigeminal nerve on the affected side were dramatically decreased when compared with those on the unaffected side, whereas FA values of the trigeminal nerves on both sides of healthy controls were not significantly different. The studies by Liu et al^[12] and Neetu et al^[13] showed similar conclusions. All these studies investigated morphological and pathological changes of the cisternal segment of the trigeminal nerve.

The parapharyngeal space, pterygopalatine fossa, and masticator space remain the most common sites for the development of NPC. The V3 branch of the trigeminal nerve leaves the cranium through the foramen ovale and then runs along the space between the tensor veli palatini and lateral pterygoid; thus, it is easily infringed upon by tumors in NPC. The applications of DTI for the extracranial segment of the trigeminal nerve have not been reported on. With respect to the imaging parameters, we employed coronary DTI for data acquisition, which is a little different from the method used in the literature report by Herweh et al.^[11] We performed DTI scanning repeatedly and concluded that it was convenient to locate the V3 branch of the trigeminal nerve on coronal images for accurate definition of the region of interests (ROIs) for DTI parameter metrics.

Our study enrolled 52 patients with NPC with a T3 classification and unilateral infringement. According to routine MR images, direct evidence of foramen ovale or masticator space invasion was not detected. However, our results showed that in comparison to the unaffected sides and the healthy controls, FA values of the V3 branch of the trigeminal nerve on the affected sides were significantly decreased. FA represents diffusion directivity and has a close relationship with structural composition. Therefore, we infer that this result indicates demyelination

Table 2**Comparison of FA and ADC values of V3 branch of the trigeminal nerve between both sides in control group (n=30, mean±STD).**

	FA	ADC ($\times 10^{-3}$ mm ² /s)
Right side	0.58±0.18	0.86±0.38
Left side	0.58±0.20	0.86±0.40
Z	-0.083	-0.541
P	0.930	0.580

ADC=apparent diffusion coefficient, FA=fractional anisotropy, STD=standard deviation.

Table 3**Comparison of FA and ADC values of V3 branch of the trigeminal nerve between the affected side of patient group and control group (n=52 and 30, mean±STD).**

	FA	ADC ($\times 10^{-3}$ mm ² /s)
Affected side	0.50±0.19	1.06±0.45
Control group	0.58±0.18	0.86±0.39
Z	-5.315	-4.28
P	0.000	0.000

ADC=apparent diffusion coefficient, FA=fractional anisotropy, STD=standard deviation.

of fiber tracts in the V3 branch of the trigeminal nerve and axonal loss. In addition, we found that the ADC values of the V3 branch of the trigeminal nerve on the affected sides were increased remarkably over those on the unaffected sides and those in healthy controls. The ADC describes the degree of free diffusion of water molecules. Thus, we speculate that tumor compression leads to a reduction in blood perfusion in the V3 branch of the trigeminal nerve, an increase in permeability of the cell membrane, and damage to the myelin sheath, which combine to enlargement of the extracellular space and subsequent acceleration of the free diffusion of water molecules. Our study results were consistent with those of Leal et al.^[14] In addition, some researchers have analyzed neurovascular compression-induced pathological changes as a result of microstructural damage to neural fiber tracts.^[15-17] Our speculation about the pathology of microstructural damage to the V3 branch of the trigeminal nerve due to tumor infringement was basically coincident with literature reports. According to this result, invasion of the V3 branch of the trigeminal nerve was underestimated by routine MRI, while it was definite in terms of the results from DTI parameter metrics. Based on these results, we consider that the enrolled patients might harbor a potential risk of distant metastasis, and should be reclassified and their prognoses reevaluated; correspondingly, clinicians should develop different therapeutic regimens for them.

The results of this study also found that the decreasing FA rate was significantly negatively correlated with the increasing ADC rate. This result has not been mentioned in the previous literature about TN, although it was consistent with the results of other microstructural abnormalities in white matter tracts derived from central nervous system lesions.^[18-20] We believe that axonal damage and interruption of the myelin sheath are bound to cause a concurrent decrease in anisotropy and acceleration in the free diffusion of water molecules, which indirectly causes a decrease in FA and increase in the ADC.

The main limitation of our study is that DTI evidence of nerve invasion lacks a pathological correlation because nonsurgical treatment is the preferred regimen for NPC. However, in 2007, Hanna et al^[21] compared MRI-evidenced perineural invasion

Table 4**Comparison of FA and ADC values of V3 branch of the trigeminal nerve between the unaffected side of patient group and control group (n=52 and 30, mean±STD).**

	FA	ADC ($\times 10^{-3}$ mm ² /s)
Unaffected side	0.55±0.20	0.89±0.42
Control group	0.58±0.18	0.86±0.39
Z	-1.667	-0.915
P	0.095	0.360

ADC=apparent diffusion coefficient, FA=fractional anisotropy, STD=standard deviation.

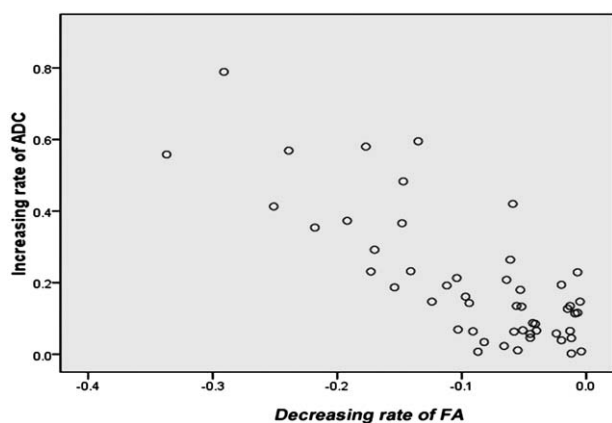


Figure 3. The correlations in the rate of change between FA and ADC values of the V3 branch of the trigeminal nerve on affected sides in patients with NPC. The decreasing FA rate was significantly and negatively correlated with the increasing ADC rate ($r = -0.675$, $P = 0.000$).

with a postoperative pathological examination and concluded that MRI had very satisfactory sensitivity (100%) and specificity (85%) for detecting the perineural spread of adenoid cystic carcinoma of the head and neck to the skull base. The study results of Gandhi et al^[22] also suggested that MRI was feasible and efficient for detecting and defining the anatomic extent of large-nerve perineural spread of malignancy. Secondly, a long-term follow-up of the patients is necessary to validate the prognostic value of DTI-evidenced nerve invasion in patients with NPC.

In conclusion, DTI parameter metrics, including FA and ADC values, can detect invasion of the V3 branch of the trigeminal nerve at an early stage in patients with NPC by reflecting microstructural abnormalities of the neural fiber tracts on the affected sides, which is meaningful for an exact T classification, scientific prognostic assessment, and determining therapeutic guidelines for patients with NPC.

References

- [1] Cao SM, Simons MJ, Qian CN. The prevalence and prevention of nasopharyngeal carcinoma in China. *Chin J Cancer* 2011;30:114–9.
- [2] Sanguineti G, Geara FB, Garden AS, et al. Carcinoma of the nasopharynx treated by radiotherapy alone: determinants of local and regional control. *Int J Radiat Oncol Biol Phys* 1997;37:985–96.
- [3] Cheng SH, Tsai SY, Horng CF, et al. A prognostic scoring system for locoregional control in nasopharyngeal carcinoma following conformal radiotherapy. *Int J Radiat Oncol Biol Phys* 2006;66:992–1003.

- [4] Cui C, Liu L, Ma J, et al. Trigeminal nerve palsy in nasopharyngeal carcinoma: correlation between clinical findings and magnetic resonance imaging. *Head Neck* 2009;31:822–8.
- [5] Liu L, Liang S, Li L, et al. Prognostic impact of magnetic resonance imaging-detected cranial nerve involvement in nasopharyngeal carcinoma. *Cancer* 2009;115:1995–2003.
- [6] Mao YP, Liang SB, Liu LZ, et al. The N staging system in nasopharyngeal carcinoma with radiation therapy oncology group guidelines for lymph node levels based on magnetic resonance imaging. *Clin Cancer Res* 2008;14:7497–503.
- [7] Edge SB, Compton CC. The American Joint Committee on Cancer: the 7th edition of the AJCC cancer staging manual and the future of TNM. *Ann Surg Oncol* 2010;17:1471–4.
- [8] Liu X, Liu LZ, Mao YP, et al. Prognostic value of magnetic resonance imaging-detected cranial nerve invasion in nasopharyngeal carcinoma. *Br J Cancer* 2014;110:1465–71.
- [9] Beaulieu C. The basis of anisotropic water diffusion in the nervous system—a technical review. *NMR Biomed* 2002;15:435–55.
- [10] Basser PJ, Pierpaoli C. Microstructural and physiological features of tissues elucidated by quantitative-diffusion-tensor MRI. *J Magn Reson* 2011;213:560–70.
- [11] Herweh C, Kress B, Rasche D, et al. Loss of anisotropy in trigeminal neuralgia revealed by diffusion tensor imaging. *Neurology* 2007;68:776–8.
- [12] Liu Y, Li J, Butzkueven H, et al. Microstructural abnormalities in the trigeminal nerves of patients with trigeminal neuralgia revealed by multiple diffusion metrics. *Eur J Radiol* 2013;82:783–6.
- [13] Neetu S, Sunil K, Ashish A, et al. Microstructural abnormalities of the trigeminal nerve by diffusion-tensor imaging in trigeminal neuralgia without neurovascular compression. *Neuroradiol J* 2016;29:13–8.
- [14] Leal PR, Roch JA, Hermier M, et al. Structural abnormalities of the trigeminal root revealed by diffusion tensor imaging in patients with trigeminal neuralgia caused by neurovascular compression: a prospective, double-blind, controlled study. *Pain* 2011;152:2357–64.
- [15] Devor M, Govrin-Lippmann R, Rappaport ZH. Mechanism of trigeminal neuralgia: an ultrastructural analysis of trigeminal root specimens obtained during microvascular decompression surgery. *J Neurosurg* 2002;96:532–43.
- [16] Hilton DA, Love S, Gradidge T, et al. Pathological findings associated with trigeminal neuralgia caused by vascular compression. *Neurosurgery* 1994;35:299–303.
- [17] Love S, Hilton DA, Coakham HB. Central demyelination of the Vth nerve root in trigeminal neuralgia associated with vascular compression. *Brain Pathol* 1998;8:1–1.
- [18] Jones DK, Lythgoe D, Horsfield MA, et al. Characterization of white matter damage in ischemic leukoaraiosis with diffusion tensor MRI. *Stroke* 1999;30:393–7.
- [19] Larsson HB, Thomsen C, Frederiksen J, et al. In vivo magnetic resonance diffusion measurement in the brain of patients with sclerosis. *Magn Reson Imaging* 1992;10:7–12.
- [20] Chabriat H, Pappata S, Poupon C, et al. Clinical severity in CADASIL related to ultrastructural damage in white matter: in vivo study with diffusion tensor MRI. *Stroke* 1999;30:2637–43.
- [21] Hanna E, Vural E, Prokopakis E, et al. The sensitivity and specificity of high-resolution imaging in evaluating perineural spread of adenoid cystic carcinoma to the skull base. *Arch Otolaryngol Head Neck Surg* 2007;133:541–5.
- [22] Gandhi MR, Panizza B, Kennedy D. Detecting and defining the anatomic extent of large nerve perineural spread of malignancy: comparing “targeted” MRI with the histologic findings following surgery. *Head Neck* 2011;33:469–75.